



## Effects of Wind on Multirotor UAS Noise Measurements

Session: Measurement Techniques - Field

EzzEldin ElSharkawy, Penn State University, USA, [ee5254@psu.edu](mailto:ee5254@psu.edu)  
Vitor T. Valente, Penn State University, USA, [vitor.valente@psu.edu](mailto:vitor.valente@psu.edu)  
Joel Rachaprolu, Penn State University, USA, [rachaprolu@psu.edu](mailto:rachaprolu@psu.edu)  
Eric Greenwood, Penn State University, USA, [eric.greenwood@psu.edu](mailto:eric.greenwood@psu.edu)

**Abstract** The aerodynamic and acoustic state of an aircraft depends strongly on its airspeed; however, most small multirotor Uncrewed Aerial Systems (UAS), or “drones,” fly autonomously using a fixed ground speed measured using onboard inertial sensors. In this work, a specially instrumented UAS with an air data system based on an ultrasonic anemometer that has been calibrated for installation effects is used to obtain accurate measurements of the airspeed and wind speed during forward flight. This UAS is used along with a ground-based acoustic array to investigate the correlation between ground speed, airspeed, and wind speed on the sound exposure level and equivalent level during flyovers. Increases in airspeed and ground speed are both found to result in a reduction in the sound exposure level, but an increase in the equivalent level. This indicates that although an increase in flight speed increases noise generation, the reduced duration of the flyover still results in a decrease in sound exposure. The flyover noise metrics were not shown to be significantly affected by wind over the range of low wind speeds tested (below 2.3 m/s).

### 1. INTRODUCTION

Aircraft noise measurements are typically conducted with the flight condition of the aircraft defined, in part, by the indicated airspeed measured by the aircraft's instruments, since the indicated airspeed has a strong effect on the aerodynamic and acoustic state of the vehicle. However, small multirotor Uncrewed Aerial Systems (UAS), or drones, introduce new challenges for acoustic measurement. Unlike conventional aircraft, small UAS typically use Global Positioning System (GPS) and other inertial sensors to fly at defined ground speeds, which can result in significant discrepancies between the commanded ground speed and actual airspeed in the presence of wind. Due to the small size of these aircraft, and the difficulty in obtaining accurate airspeed measurements at low flight speeds using conventional Pitot probes, it is not common for small multirotor UAS to be equipped with air data systems. However, because these vehicles fly at low flight speeds, even relatively low wind

velocities can lead to large differences between the airspeed and ground speed of the aircraft. Consequently, the effect of wind on the generation of noise by these vehicles is not well understood.

Prior research by Go and Choi (Go & Choi, 2024) demonstrated how wind interactions modify the noise footprint of multi-rotor drones during flight, underscoring the importance of accurate airspeed and wind direction measurements in acoustic analyses. Additionally, as noted by Zhou et al. (Zhou, Jiang, & Huang, 2022), wind and atmospheric turbulence cause frequent variations in propeller RPM to maintain flight stability. This leads to fluctuations in the Blade Passing Frequency (BPF) and alters the noise generation of UAS. Ramos-Romero et al. (Ramos-Romero, Green, Torija, & Asensio, 2023) have also emphasized the importance of monitoring weather conditions, particularly wind speed and direction, as these factors critically influence the noise emissions of small UAS during flight. In many cases, researchers have sought to conduct acoustic measurements under near zero wind conditions (Alexander & Whelchel, 2019; Škultéty, Bujna, Janovec, & Kandra, 2023); however, it may be difficult to assure that wind speeds measured from the ground are representative of those at the flight altitude of the vehicle.

The objective of this paper is to conduct an initial investigation of the effects of wind on small multirotor UAS noise measurements. Using a specially instrumented UAS with a calibrated air data system, flyover noise measurements are collected under varied commanded ground speeds, wind speeds, and wind directions.

## **2. METHODOLOGY**

This section first describes the experimental approach used in this research, including the test site and acoustic array configuration, the configuration of the UAS and its instrumentation, and the specific flight procedures used to collect the data. Next, the data analysis methods used to produce the results are described.

### **2.1 Acoustic Data Collection**

The acoustic data were collected at Mid-State Regional Airport (KPSB) in Phillipsburg, Pennsylvania. This test site is characterized by its remote location and low background noise levels, making it an ideal environment for acoustic measurements. The acoustic array was deployed over a grassy area off of the end of one of the runways.

The acoustic array consists of nine microphones arranged as two perpendicular linear arrays each made up of 5 microphones as shown in Fig. 1. Microphones 1 to 5 are aligned from west to east, and microphones 6 to 9 are aligned from south to north, with microphone 3 being the central microphone for both axes. Each leg of the microphone array spans 61 meters. This layout allows for multiple points where the aircraft is directly above the microphone.

Inverted ground plane microphones were installed over a reflective 40 cm diameter circular steel plate, per SAE ARP 4055 (SAE International, 1988). Additionally, the microphones are covered with windscreens to reduce the effect of wind noise. The approach used is detailed in (Konzel & Greenwood, 2022).

Acoustic data acquisition was performed using a battery-powered, field-deployable system capable of simultaneous sampling across up to 36 channels at a rate of 131 kHz with 24-bit resolution. For this study, a sampling rate of 65 kHz was employed. Additionally, GPS time data was utilized to achieve sub-sample accurate time synchronization between the acoustic measurements and the aircraft state data.

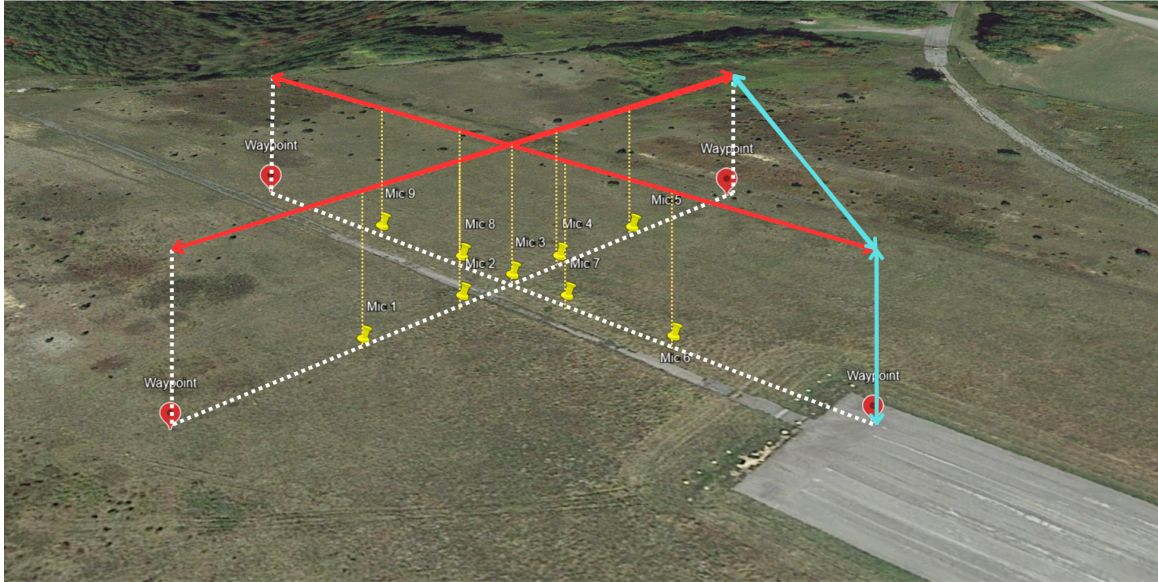


**Figure 1:** Measurement flight path (red) and microphone locations (yellow). The cyan path shows the route to and from the takeoff location.

## 2.2 UAS Configuration

The UAS utilized in this study is a custom-built reconfigurable multirotor UAS, configured in this study as a hexacopter, that was specifically designed to support noise measurement research. The aircraft is shown in Figure 2. The aircraft's frame is constructed entirely from carbon fiber, to provide payload capacity for research instrumentation. As configured in this study, the UAS has an approximate takeoff weight of 18 kg.



**Figure 2:** Custom UAS mid-flight test.

The vehicle is roughly 1.7 meters in diameter, excluding the propellers, with motor arms extending approximately 0.53 meters. The total height at the center of the main body frame is 0.28 meters. The propulsion system consists of six Vertiq 8108 brushless motors, each equipped with 71x23 cm (28x9.2 inch) carbon fiber propellers attached via a quick-attach mechanism for easy maintenance and replacement. The motors are each equipped with encoders, to allow the rotor shaft speed and position to be measured during flight.

The avionics suite is built around a PX4-compatible flight control board, complemented

by a real-time kinematic differential GPS (RTK-DGPS) system that provides centimeter-accurate positioning and timing data. The UAS is powered by two 6S batteries, each with a capacity of 22,000 mAh, configured for 12S operation to maximize flight performance and duration. More details of the aircraft and its configuration are described in (Valente, Greenwood, & Johnson, 2023).

For this study, the UAS was fitted with an Airmar WS-150WX weather station, mounted above the vehicle's center to minimize rotor-induced airflow distortions. This system is connected to an onboard computer and sampled at approximately 5 Hz, providing critical measurements such as wind speed, direction, air temperature, static pressure, and relative humidity. This system is also equipped with its own dedicated external GPS system to allow for the synchronization of air data with all other data. Following the approach described in (ElSharkawy, Valente, Rachaprolu, & Greenwood, 2024), the air data system was calibrated to produce an accurate measure of the true airspeed of the aircraft, accounting for the aerodynamic installation effects caused by the flowfield around the vehicle while in forward flight.

### 2.3 Flight Procedures

The flight path was pre-planned and programmed at the ground control station, then unloaded to the onboard computer. The flight path flies over and along the two microphone arrays, with two perpendicular flyovers each being flown along both directions, for four passes over the center of the array for each run. Each section of the run is 122 meters long as to give the aircraft 30 meters to reach a steady state before flying over the first microphone, and 30 meters of distance to slow back down and come to a complete stop before performing a 180-degree yaw maneuver. Flying in four directions allows for capturing data under varying wind conditions including upwind, downwind, and both crosswinds.

The acoustic and wind speed measurements were conducted at five different ground speeds, as shown in Table 1. These measurements follow the pattern discussed earlier in the document.

**Table 1:** Ground speeds for acoustic and wind speed measurements.

Ground Speed (m/s)
2
4
6
8
10

Data collection was repeated at various times over multiple test days, so as to acquire data under varied wind conditions.

### 2.4 Data Processing

This section describes the data processing procedure followed in this paper, as illustrated in Figure 3.

The first step in the data processing workflow involves loading raw air data collected from the weather station. Raw air data is processed into data structure that includes the wind direction, temperature, pressure, humidity, GPS time and position, and airspeed. Due to the different sampling rates of each variable measured in the weather station, each measurement is associated with its own unique time vector. This ensures that all data points are accurately timestamped according to their respective collection times.

The next step involves applying the calibration curve generated using the process outlined in (ElSharkawy et al., 2024) to correct the airspeed measured by the air data system

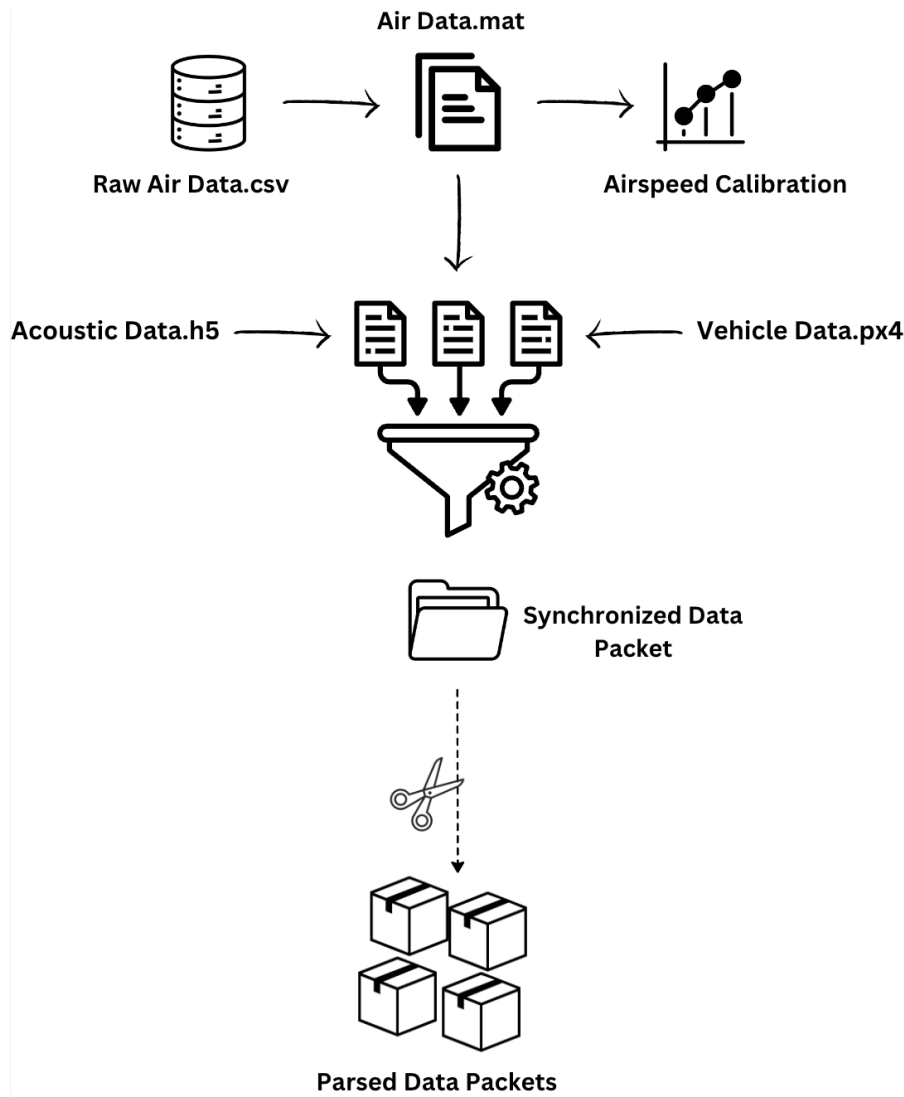


**Figure 3:** Flowchart of the data processing workflow.

to a true airspeed that accounts for effect of the flow field around the aircraft and probe. Once the calibrated true airspeed is obtained, the wind speed can be determined from the difference between the measured airspeed vector and the ground speed.

Next, the acoustic data are synchronized to the previous weather station and vehicle data. This synchronization process utilizes GPS time ensuring temporal consistency across all data sources. The synchronized data is then compiled into a structured file, facilitating further analysis.

Once the data are synchronized, the next step involves parsing the data by determining specific time windows based on the aircraft's position relative to the microphones. The process begins by identifying the moment when the aircraft is closest to the first microphone in the sequence, which serves as a reference point. Using the known distance from the starting point to the first microphone and the aircraft's speed, the amount of time required for the aircraft to cover that distance is calculated. The time window is then extended backward from the reference point by this calculated duration to capture the approach to the microphone. Similarly, the time window is extended forward after the aircraft passes the last microphone to include the departure from the area of interest. This approach captures the full duration of the aircraft's passage over the microphones, allowing time-integrated acoustic measurements to be calculated for each microphone under the flight path for each test run.



The final stage of data processing the acoustic metrics for each flyover pass. First, the A-weighted Sound Pressure Level (SPL) time history is computed. Next, the peak SPL during the pass is identified, along with the points in time before and after the peak that are 10 dB below the peak level. These time points define the duration,  $T$ , over which the acoustic metrics are computed for the flyover. The equivalent level,  $L_{eq}$  is computed as:

$$L_{eq} = 10 \log_{10} \left( \frac{1}{M} \sum_{j=1}^M 10^{\frac{SPL_j}{10}} \right) \quad (1)$$

where  $M$  is the number of data points within the selected time range, and  $SPL_j$  is the A-weighted SPL at time point  $j$ .

From the equivalent level, the Sound Exposure Level (SEL) can be computed by accounting for the duration of the flyover:

$$SEL = L_{eq} + 10 \log_{10}(T) \quad (2)$$

With the  $L_{eq}$  and SEL determined, these metrics are then compared to the variation in the average ground speed, airspeed, and wind speed measured during each flyover pass to identify linear correlations between the speeds and the resulting noise metrics.

Figure 4 provides an example of the data analyzed for each flyover pass. The upper plot depicts the ground speed and airspeed measured during the flyover pass, and the lower plot the variation in SPL over the same time. The bold portions of all three plots indicate the window of data within 10 dB of the peak SPL used in the analysis. Over this window of time, the ground and airspeed are averaged to produce a single value for each, and the difference is used to compute an averaged wind speed. As expected, the ground speed is steady, since the vehicle is programmed to fly at a constant ground speed, whereas there are small variations in the airspeed over this time window. The acoustic data are likewise integrated to compute the  $L_{eq}$  and SEL metrics over the time window. Data from this example are derived from a 2 m/s run headed east with acoustic data from microphone 3.

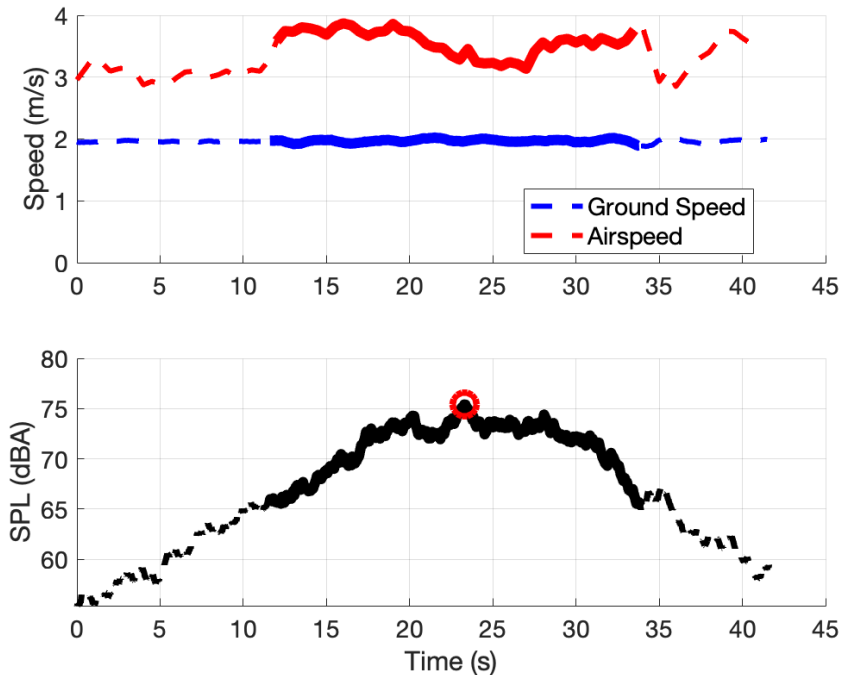


**Figure 4:** Airspeed, ground speed, and SPL for 2 m/s eastbound flight.

### 3. RESULTS AND DISCUSSION

This section presents the analysis of acoustic and flight data, focusing on the relationship between Airspeed (AS), Ground Speed (GS), Wind Speed (WS), equivalent level ( $L_{eq}$ ), and Sound Exposure Level (SEL). Negative wind speed values indicate a tailwind while positive wind speeds indicate a headwind. Also note that color of each marker indicates the aircraft's airspeed, as measured by the air data system and averaged over the selected time window.

The relationship between ground speed and SEL is shown in Figure 5. Clusters of data points occur at each of the commanded ground speeds flown during the test. While there is significant variation in the SEL for each ground speed, there is a general trend of reduced SEL with increasing ground speed. Fitting a linear best-fit curve to all available data, as the ground speed increases by 1 meter per second, the SEL decreases by 0.63 dB. The coefficient of determination,  $R^2$ , has a value of 0.70 indicating a relatively strong correlation between ground speed and SEL. This is consistent with trends previously observed by (Konzel & Greenwood, 2022).

Figure 6 illustrates the impact of airspeed on SEL. Due to the variation in the wind speed and direction, the measured airspeeds vary between runs with the same ground speed set point. As with ground speed, the SEL decreases with increasing airspeed. With an increase in airspeed of 1 meter per second, the SEL decreases by 0.52 dB. The  $R^2$  value of 0.48 suggests a moderate correlation.

Figure 7 shows the relationship between wind speed and SEL. A best fit curve indicates an increase in SEL by 0.57 dB for every meter-per-second increase in wind speed along the flight direction. This is comparable to the effect of changing the airspeed of the aircraft. However, since the variation in flight speeds is much greater than the variation in wind speeds, there is considerable scatter in these data. This results in a relatively low correlation coefficient,  $R^2 = 0.12$ .

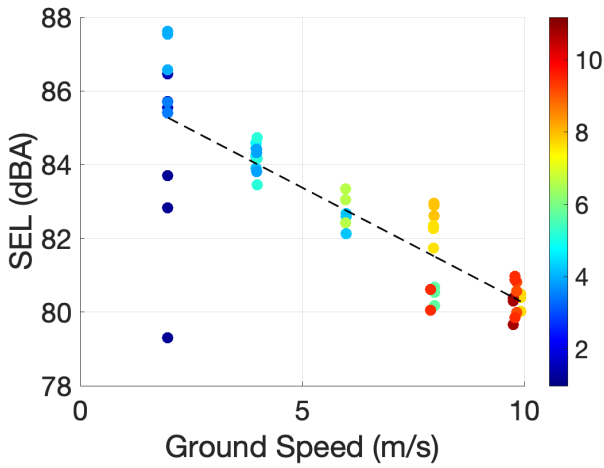
The trend in SEL with the flight speed of the vehicle may be attributed to the increase in ground speed reducing the duration of sound exposure, decreasing the SEL. In order to look at how changes in flight speed affect noise generation at the source, the same analysis is conducted using the equivalent level,  $L_{eq}$ , to account for the varying duration of flyovers at different speeds. Figure 8 plots the variation in  $L_{eq}$  with ground speed. Unlike the trend with SEL, increasing ground speed is associated with an increase in the equivalent level. The  $L_{eq}$  increases by 0.29 dB for each meter per second increase in ground speed. This positive slope indicates that the noise generated by the aircraft increases with faster ground speeds. However, the  $R^2$  value of 0.25 suggests a weaker correlation than that found for SEL.

Figure 9 shows the variation in equivalent sound level with airspeed. The shows a similar trend to the ground speed, with  $L_{eq}$  also increasing by 0.29 dB per meter per second of airspeed. The  $R^2$  value of 0.25 again indicates a relatively weak correlation.

The variation in  $L_{eq}$  with wind speed is plotted in Figure 10. In this case, there is no clear trend between the equivalent level and the wind speed, with the correlation coefficient approaching zero.

### 4. CONCLUSION

This study described a preliminary exploration of the impact of wind on noise measurements for multirotor Uncrewed Aerial Systems (UAS) using a calibrated air data system. The results indicate that both ground speed and airspeed significantly influence ground noise metrics during flyover. The sound exposure level is found to decrease with increasing flight speed, whereas the equivalent level increases with increasing flight speed. This suggests that although the noise generation of the aircraft does increase as the speed of the aircraft increases, this has a smaller effect on the sound exposure level than the reduction in



**Figure 5:** Ground speed vs. SEL.

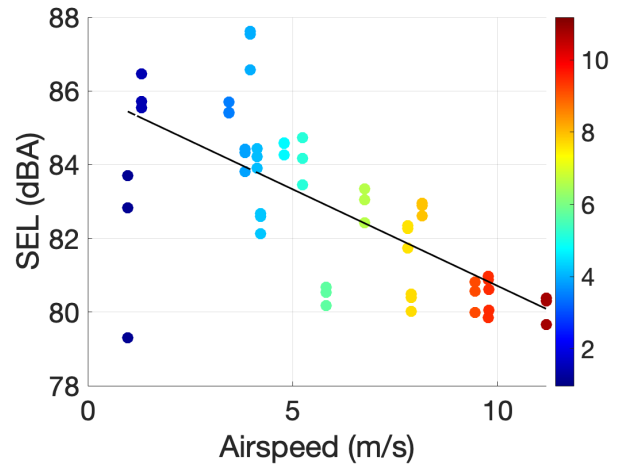


**Figure 6:** Airspeed vs. SEL.

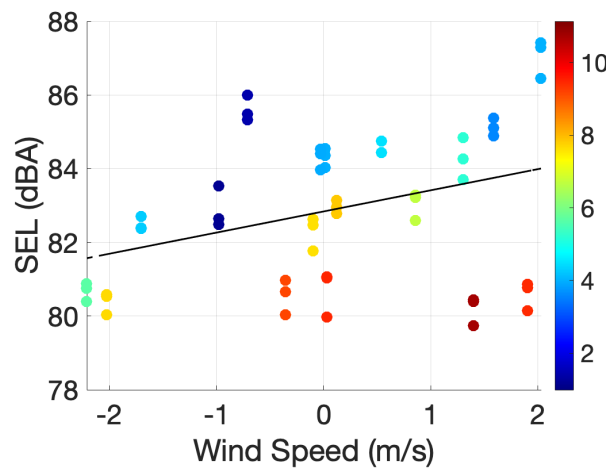


**Figure 7:** Wind speed vs. SEL.

duration with increasing flight speed. The correlation between SEL and ground speed is somewhat stronger than the correlation between SEL and airspeed, which can be expected since the variation in SEL is primarily due to the change in duration. However, the variation in noise metrics is generally consistent regardless of whether airspeed or ground speed is used to define the flight condition. Likewise, the wind speed was not strongly correlated with either noise metric. It was observed that tailwinds resulted in lower SEL, while headwinds increased SEL, but no significant correlation was found with  $L_{eq}$ . However, it should be noted that the wind speeds captured in the present study varied between 0 and 2.2 m/s. Higher wind speeds are likely to have a more significant impact on the measured noise. In future flights, data will be collected under higher wind conditions, with the aim of establishing wind speed limits for repeatable acoustic data collection.

## ACKNOWLEDGMENTS

This research was funded by the U.S. Federal Aviation Administration Office of Environment and Energy (AEE) through ASCENT, the FAA Center of Excellence for Alternative Jet Fuels and the Environment, Project 77 through FAA Award Number 13-C-AJFE-PSU Amendment No. 112 managed by Dr. Hua (Bill) He of AEE. Any opinions, findings, conclusions, or recommendations expressed in this material are those of the authors and do not necessarily reflect the views of the FAA.



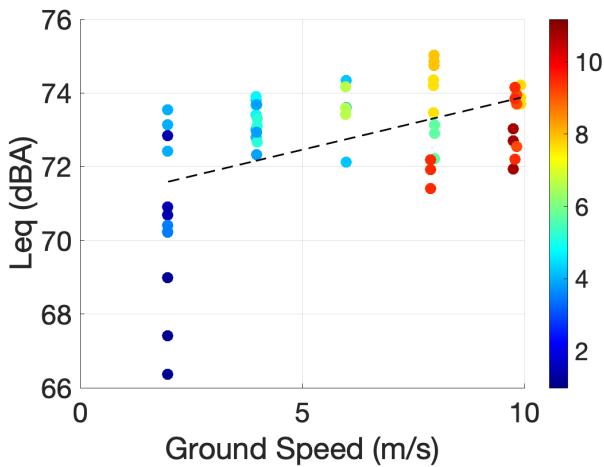


**Figure 8:** Ground Speed vs. Leq

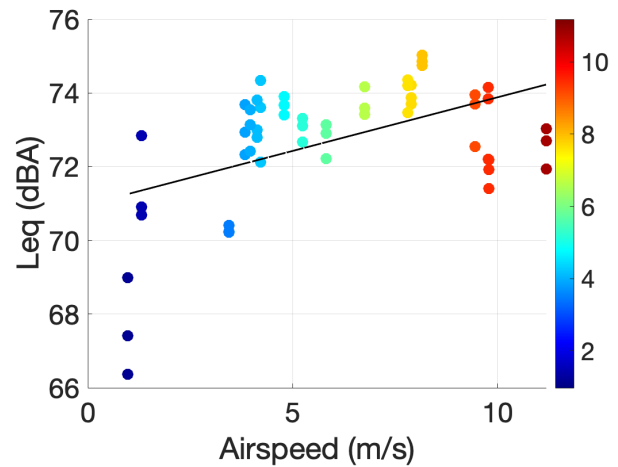


**Figure 9:** Airspeed vs. Leq

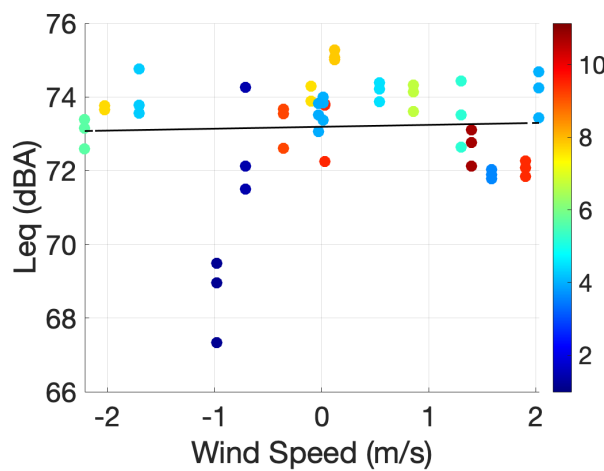


**Figure 10:** Wind Speed vs. Leq

## REFERENCES

- Alexander, W. N., & Whelchel, J. (2019, June). Flyover noise of multi-rotor suas. In *Proceedings of Inter-Noise 2019* (p. 1502-1512). Blacksburg, VA, USA.
- ElSharkawy, E., Valente, V. T., Rachaprolu, J. S., & Greenwood, E. (2024, July). Calibration of an air data system for small multirotor aircraft. In *AIAA Aviation Forum and ASCEND 2024*. doi: 10.2514/6.2024-4393
- Go, Y., & Choi, J. (2024, April). An investigation of multi-rotor drone noise based on the acoustic hemisphere in an actual environment. *International Journal of Aeronautical and Space Sciences*, 25, 420-434. doi: 10.1007/s42405-023-00697-y
- Konzel, N. B., & Greenwood, E. (2022, May). Ground-based acoustic measurements of small multirotor aircraft. In *Proceedings of the 78th Annual Forum of the Vertical Flight Society*. doi: 10.4050/F-0078-2022-17435
- Ramos-Romero, C., Green, N., Torija, A. J., & Asensio, C. (2023, October). On-field noise measurements and acoustic characterisation of multi-rotor small unmanned aerial systems. *Aerospace Science and Technology*, 141. doi: 10.1016/j.ast.2023.108537
- SAE International. (1988, Jan). *Ground-plane microphone configuration for propeller-driven light-aircraft noise measurement*. Aerospace Recommend Practice 4055.
- Valente, V. T., Greenwood, E., & Johnson, E. N. (2023, May). An Experimental Investigation of eVTOL Flight State Variance on Noise. In *Proceedings of the 79th Annual Forum of the Vertical Flight Society*.
- Zhou, T., Jiang, H., & Huang, B. (2022, May). Quad-copter noise measurements under

realistic flight conditions. *Aerospace Science and Technology*, 124. doi: 10.1016/j.ast.2022.107542

Škultéty, F., Bujna, E., Janovec, M., & Kandra, B. (2023, May). Noise impact assessment of uas operation in urbanised areas: Field measurements and a simulation. *Drones*, 7(5). doi: 10.3390/drones7050314

## Technical Report Documentation Page

1. Report No.	2. Government Accession No.	3. Recipient's Catalog No.	
4. Title and Subtitle		5. Report Date	
		6. Performing Organization Code	
7. Author(s)		8. Performing Organization Report No.	
9. Performing Organization Name and Address		10. Work Unit No. (TRAIS)	
		11. Contract or Grant No.	
12. Sponsoring Agency Name and Address		13. Type of Report and Period Covered	
		14. Sponsoring Agency Code	
15. Supplementary Notes			
16. Abstract			
17. Key Words		18. Distribution Statement	
19. Security Classif. (of this report) Unclassified	20. Security Classif. (of this page) Unclassified	21. No. of Pages	22. Price